Figure 5 (a) Picture, (b) simulated and measured frequency response, and (c) group delay of the fabricated BPF with the MTZS

center frequency. The size is also smaller than about $0.26\lambda_g$ by $0.32\lambda_g$, e.g., in Ref. 5. Although the measured results are slightly different with the simulated results in the upper band, which can be considered as the material dispersion, the proposed filter still shows a good potential for the broadband communications. In addition, it can be realized on the low-cost FR4 substrate without using expensive lithography process or high-cost commercial substrate [3-6].

4. CONCLUSIONS

In this article, a compact UWB bandpass filter having a wide stopband is reported. A PI-WBF is used as the prototype filter and a MTZS, connected to the output port of the PI-WBF, acting as a bandstop filter to provide the multiple transmission zeros with asymmetrical locations to widen upper stopband of the PI-WBF. This designed filter at 4 GHz was fabricated and measured, showing good characteristics. The proposed filter is very useful because

of its simple design, high performances, and easy fabrication without expensive lithography process.

REFERENCES

1. IEEE P802.15 Working group for wireless personal area networks, detailed DS-UWB simulation results, IEEE 802.15-04-0483r4 (2004), 11-12.
2. C.Y. Hung, M.H. Weng, Y.K. Su, R.Y. Yang, and H.W. Wu, Design of sharp-rejection, compact and low-cost ultra-wideband bandpass filters using interdigital resonators, Microwave Opt Technol Lett, 48 (2006), 2093-2096.
3. G.G. Roberto and I.A. José, Design of sharp-rejection and low-loss wide-band planar filters using signal-interference techniques, IEEE Trans Microwave Theory Tech 15 (2005), 530-532.
4. L. Zhu, S. Sun, and W. Menzel, Ultra-wideband (UWB) bandpass filters using multiple-mode resonator, IEEE Microwave Wireless Compon Lett 15 (2005), 796-798.
5. K.M. Shum, W.T. Luk, C.H. Chan, and Q. Xue, A UWB bandpass filter with two transmission zeros using a single stub with CMRC, IEEE Microwave Wireless Compon Lett 17 (2007), 43-45.
6. P. Mondal and A. Chakrabarty, Compact wideband bandpass filters with wide upper stopband, IEEE Microwave Wireless Compon Lett 17 (2007), 31-33.
7. M.Y. Hsieh and S.M. Wang, Compact and wideband microstrip bandstop filter, IEEE Microwave Wireless Compon Lett 15 (2005), 472-474.
8. Zelad Software, IE3D Simulator, (1997).

© 2007 Wiley Periodicals, Inc.

EMISSION CHARACTERISTICS OF NEAR-ULTRAVIOLET TWO-DIMENSIONAL ORGANIC PHOTONIC CRYSTAL LASERS

Ying Dong,[1] Junfeng Song,[1] Chuanhui Cheng,[1] Wenhai Jiang,[1] Shukun Yu,[1] Guotong Du,[1,2] and Xu Wang[3]
[1] State Key Laboratory on Integrated Optoelectronics, College of Electronic Science and Engineering, Jilin University, Qianjin Street 2699, Changchun 130012, China; Corresponding author: dongyingnancy@yahoo.com.cn
[2] State Key Laboratory of Materials Modification by Laser, Ion, and Electron Beams, Department of Physics, Dalian University of Technology, Dalian 116023, China
[3] The Key Laboratory for Supramolecular Structure and Materials of Ministry of Education, Jinlin University, Qianjin Street 2699, Changchun 130012, China

ABSTRACT: *We demonstrate near-ultraviolet frequency two-dimensional organic-photonic-crystal laser using resonator structures that offer two-dimensional distributed feedback at room temperature. The gain medium is N,N'-di-1-naphthyl-N, N'-diphenylbenzidine (NPB) which is deposited on lithographically patterned silica structure. We observe surface emitting lasing action with the central beam normal to the surface and the far-field emission characteristics of this laser. The devices operate in the blue spectral region, and exhibit very low threshold energies for oscillation (0.3 kW/cm^2). The far field is also shown to contain information about the quality of the photonic crystal. This emission pattern offers a convenient and powerful way to evaluate the nature of laser action in such resonators. © 2007 Wiley Periodicals, Inc.*

1. INTRODUCTION

Photonic crystals exhibit many interesting properties such as photonic band gap (PBG) and defect modes [1].Using of photonic crystals (PCs) as laser resonator has been advocated because photonic band gap materials are able to modify the density of electromagnetic modes and thus enhance or suppress spontaneous emission [2]. The interaction between the light and the matter has realized nanoscale lasers [3], Rabi splitting [4], and photon trapping [5]. PCs with a nanocavity will improve the device properties using their resonant modes. There have also been reports on the lasing operation of two-dimensional (2D) PCs with organic molecules and semiconductor gain materials [6-8]. The principal reason for this is that, in many cases, it is relatively easy for fabricating lasers with solid-state organic gain media. Using organic molecules as active materials of PCs lasers will pave the way for the utilization of PCs in chemistry beyond physics [9]. 2D photonic crystal structures with organic layers have observed no photonic band gap in the plane [8, 10]. Recently, there has been a lot of study in 2D surface-emitting PCs lasers utilizing a 2D distributed feedback (DFB) mechanism [6-8, 11, 12].

Distributed feedback (DFB) has been proven to be particularly useful for organic semiconductor devices as it allows low threshold lasing in thin film waveguide structures [12, 13]. Instead of one-dimensional (1D) feedback gratings, two-dimensional (2D) PCs can be used, potentially resulting in lower lasing threshold and highly directional vertically emitting structures [14]. The conventional DFB semiconductor laser is a first-order grating, providing feedback in the plane. The second-order DFB laser has the same emission pattern as the first order laser and besides, emission perpendicular to the plane [15]. The vertical emission light from several superimposed linear grating interferes constructively perpendicular to the plane defined by the 2D PCs structure.

In this article, we demonstrate near-ultraviolet frequency two-dimensional organic-photonic-crystal laser at room temperature. The photonic crystals possess honeycomb symmetries. The silica
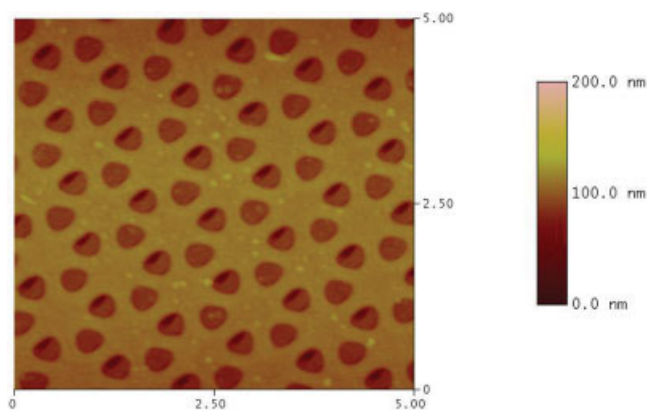

Figure 1 AFM of a honeycomb lattice photonic crystal laser. [Color figure can be viewed in the online issue, which is available at www.interscience.wiley.com]
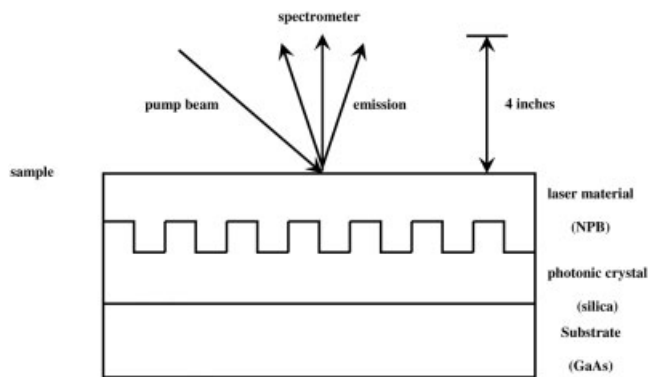

Figure 2 A schematic representation of the laser structure

microstructured substrate that provide distributed feedback is fabricated by photolithographically, which is etched to form a two-dimensional surface relief pattern of 60–80 nm depth. Each pattern is 75 μm $\times$ 75 μm on one chip. The lattice constant $a = 500$ nm and hole cylinder radius $r = 130$ nm. The gain medium N,N'-di-1-naphthyl-N, N'-diphenylbenzidine (NPB) is deposited by vacuum ($<1.0 \times 10^{-3}$ Pa) thermal evaporation. The thicknesses of NPB are in the range of 200–250 nm. A top view atomic force micrograph (AFM) of a part of one pattern is shown in Figure 1.

A schematic representation of the laser structure is shown in Figure 2. The GaAs is the substrate. The silica-NPB-air structures form asymmetric planar waveguides that support only the fundamental transverse electric mode. NPB acts as gain medium and is optically pumped. NPB shows strong, low threshold stimulated emission in the blue spectral region and exhibit large optical gain coupled with low loss in slab waveguide geometries. Resonant feedback in the guides is induced by the photonic crystals, which couples counter propagating waves within the film plane. The direction of light output from the plane is determined by phase matching the scattered wave to the guided wave. The laser features emission perpendicular to the plane of the photonic crystal. The vertically emitted light from the superimposed gratings interferes constructively perpendicular to the plane defined by the grating directions. For large area photonic crystal structures, this results in highly directional radiation out of plane of the photonic crystal [7]. It is carefully chosen so that feedback could be achieved at wavelength with the gain region of NPB and for sufficiently thin organic layer that all higher order longitudinal modes are suppressed. In our DFB lasers, optical feedback is provided through second-order Bragg scattering of the waveguide radiation, while the laser beam is output-coupled by second-order scattering, which supports radiation in a direction perpendicular to the substrate (surface emission). It is important to note that a film patterned with a photonic crystal structure will produce a photoluminescence (PL) spectrum that has an angular dependence due to the diffraction process in the photonic crystal. Therefore, care must be taken to avoid misinterpreting the PL spectrum. To test the directionality of the emission, the laser spectrum was recorded at 4 in. away from the sample.

The absorption and emission spectrum of NPB are given in Figure 3. The inset of Figure 3 shows the chemical structure of NPB. The absorption spectrum features maximal at 352 nm and the neat film photoluminescence spectrum features maximal at 438 nm. The gain material has an index of ~1.75 at this wavelength.

Using a continuous He-Cd laser operating at 325 nm, we focused about 1.06 kW/cm^2 power density on the sample surface
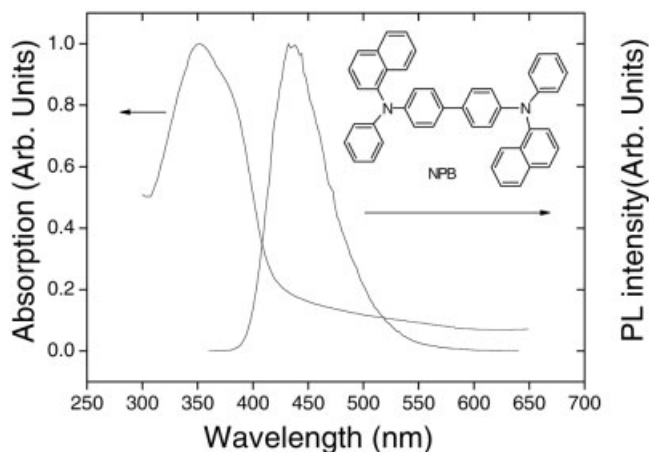
Figure 3 Absorption spectra and photoluminescence spectra of neat NPB film (excited using the 325 nm line from an He-Cd laser). The inset shows the chemical structure of NPB

at normal incidence in an estimated 60 μm spot size with a convex lens in this experiment. The lasing threshold for this device is much lower than that photonic crystal-based organic lasers reported in literature. We observed a sharp lasing peak whose lasing wavelength is about 409 nm. The full width at half maximum is limited by the resolution of the spectrometer which is about 2 Å. The results are summarized in Figure 4. We did not observe lasing for areas without a photonic crystal pattern under the same pumping condition. The emission from the structured site features significant spectral narrowing at the resonance wavelength of the DFB structure. The observed laser emission was normal to the surface of the device. One nonlasing peak was observed in the spectrum, as shown in Figure 4. We think one possibility is that other resonant peaks near the band edge are created by a little amount of deformation or imperfection in the real sample. Figure 5 shows the effect of increasing the pump energy, and the associated rise in the laser peak, as it becomes the dominant the feature in the spectrum.

Figure 6 shows the measured light density as a function of incident pump power. A clear threshold near 0.3 kW/cm^2 is observed. The inset of Figure 6 is the far-field image of one honeycomb lattice laser in which is the image of the emission
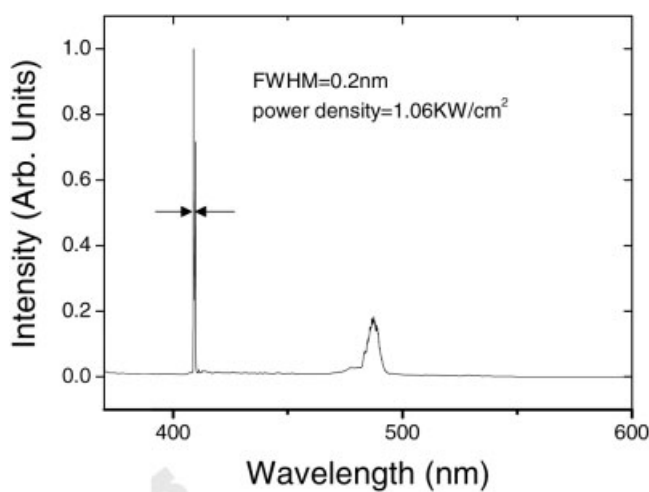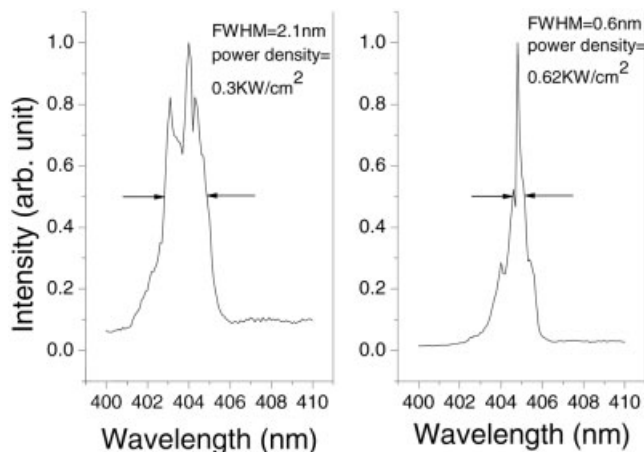

Figure 5 Emission spectra for pump energies above and below laser threshold

from the sample with lattice constant a = 500 nm and hole radius r = 130 nm. These images were obtained by digital camera of light incident upon an ultraviolet sensitivity paper placed about 3–5 cm from the laser. The details of the far-field image provide considerable insight into the nature of laser action in these structures. The observed emission is generated in the plane of the waveguide and subsequently diffractively coupled out of plane, facilitating imaging.

Laser action in these structures arises principally because of Bragg reflections induced by the periodicity of the photonic lattice, which causes the density of photon states to peak and the group velocity of photons to reach zero along certain high-symmetry directions in k space. The resulting feedback gives rise to laser action. In k space, for a honeycomb lattice, there are six M high-symmetry points in the Brillouin zone corresponding to the mid points of six sides of a regular hexagon. In real space, laser action will be directed along six corresponding directions in the plane of the waveguide. As a result of diffractive coupling, some of the laser emission is scattered out of plane of the waveguide. The ideal far-field image should be six spots forming a hexagon.
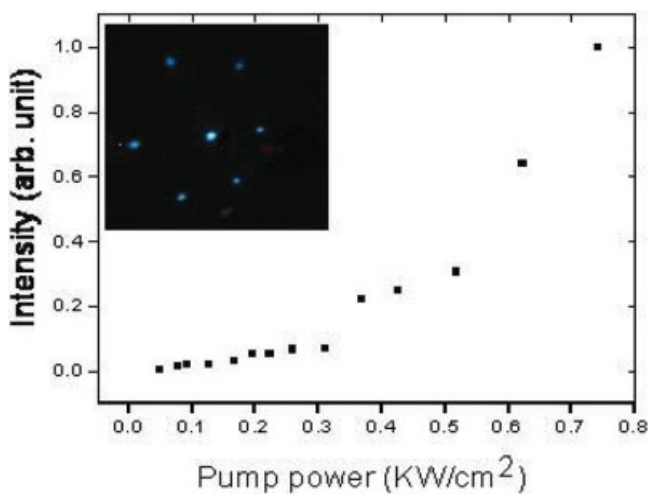

Figure 4 Laser emission spectrum from a honeycomb photonic crystal laser

Figure 6 Measured emission power from one of the photonic crystal laser as a function of incident pump power. A clear lasing threshold near 0.30 kW/cm^2 can be observed. The inset shows the far-field emission of one two-dimensional photonic crystal laser. [Color figure can be viewed in the online issue, which is available at www.interscience.wiley.com]
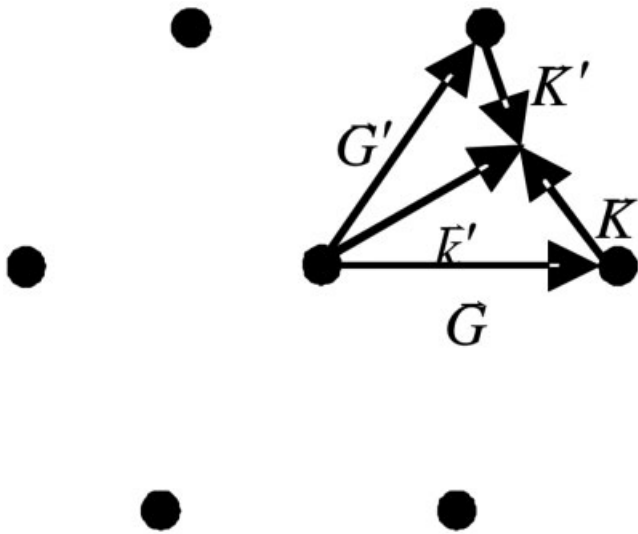
Figure 7 Reciprocal lattice for a 2D grating. Shown are the guided-mode wave vector **k**, two possible reciprocal lattice vectors **G** and **G′**, that satisfy the phase-matching condition, and the in-plane components of the two corresponding radiation-mode wave vectors **K** and **K′**

In Figure 7 we show the phase-matching condition in a reciprocal lattice of a 2D PC coupler for a certain guided-mode wave vector. For a general 2D PC laser, we consider a grating in a planar dielectric waveguide on top of a substrate. The wave vector of the waveguided mode that is incident upon the grating section be **k**, it's free-space wavelength λ, the in-plane component of the scattered radiation wave vector **K**, and the polar angle of the output direction θ. If the number of periods in the grating is enough large, the field scattered by the grating will interfere constructively only in certain direction. The phase-matching condition is $\mathbf{k} = \mathbf{K} + \mathbf{G}$, where **G** is a reciprocal lattice vector. The emitted radiation is in two directions, **K** and **K′**, so this grating acts as a two-way splitter. Light is emitted into one half-space into two directions, with different azimuthal and polar angles.

The grating has a plane of symmetry that is perpendicular to the propagation direction. The two propagating modes combine to give a mode that is symmetric and one that is asymmetric with respect to reflection through this plane. The asymmetric mode cannot couple to free-space plane waves, so no energy is lost from the slab when this mode is excited. The symmetric mode loses energy at twice the rate of the propagating mode. In two-dimensional gratings, four modes, or even six modes in a honeycomb lattice can mix.

In conclusion, we have reported the characteristics of novel lasers with organic thin-film gain media. Laser action arises from two-dimensional distributed feedback from a honeycomb photonic crystal. We studied the laser action from two-dimensional photonic crystal instabilities associated with pumping geometry for the two-dimensional case. We described the far-field characteristics of these lasers. Laser action is a result of the group velocity of photons reaching zero at certain high-symmetry points in the Brillouin zone. This leads to coupling between the forward and backward propagating waves (as in a distributed feedback laser) which results in laser oscillation along specific directions in real space.

REFERENCES

1. E. Yablonovitch, Inhibited spontaneous emission in solid-state physics and electronics, Phys Rev Lett 58 (1987), 2059–2062.
2. O.J. Painter, A. Husain, A. Scherer, et al., Room temperature photonic crystal defect lasers at near-infrared wavelengths in InGaAsP, J Lightwave Technol 17 (1999), 2082–2088.
3. O. Painter, R.K. Lee, A. Scherer, et al., Two-dimensional photonic band-Gap defect mode laser, Science 284 (1999), 1819–1821.
4. T. Yoshie, A. Scherer, J. Hendrickson, et al., Vacuum Rabi splitting with a single quantum dot in a photonic crystal nanocavity, Nature 432 (2004), 200–203.
5. S. Noda, A. Chutinan, and M. Imada, Trapping and emission of photons by a single defect in a photonic bandgap structure, Nature 407 (2000), 608–610.
6. M. Meier, A. Mekis, A. Dodabalapur, et al., Laser action from two-dimensional distributed feedback in photonic crystals, Appl Phys Lett 74 (1999), 7–9.
7. A. Mekis, A. Dodabalapur, R.E. Slusher, et al., Two-dimensional photonic crystal couplers for unidirectional light output, Opt Lett 25 (2000), 942–944.
8. A. Mekis, M. Meier, A. Dodabalapur, et al., Lasing mechanism in two-dimensional photonic crystal lasers, Appl Phys A 69 (1999), 111–114.
9. N. Tessler, Lasing from conjugated-polymer microcavities, Nature 382 (1996), 695.
10. R. Harbers, N. Moll, R.F. Mahrt, et al., Enhancement of the mode coupling in photonic-crystal-based organic lasers, J Opt A 7 (2005), S230–S234.
11. G.A. Turnbull, P. Andrew, W.L. Barnes et al., Photonic mode dispersion of a two-dimensional distributed feedback polymer laser, Phys Rev B 67 (2003).
12. S. Riechel, U. Lemmer, J. Feldmann, et al., Laser modes in organic solid-state distributed feedback lasers, Appl Phys B 71 (2000), 897–900.
13. H. Kogelnik, Coupled-wave theory of distributed feedback lasers, J Appl Phys 43 (1972), 2327.
14. H. Kogelnik, Stimulated emission in a periodic structure, Appl Phys Lett 18 (1971), 152.
15. K. Forberich, A. Gombert, S. Pereira et al., Lasing mechanisms in organic photonic crystal lasers with two-dimensional distributed feedback, J Appl Phys 100 (2006).